Brain Imaging and Behavior (2020) 14:857–868
https://doi.org/10.1007/s11682-018-0031-x

ORIGINAL RESEARCH

Common and specific altered amplitude of low-frequency fluctuations in Parkinson's disease patients with and without freezing of gait in different frequency bands

Huiqing Hu[1] · Jingwu Chen[2] · Huiyuan Huang[1] · Caihong Zhou[2] · Shufei Zhang[1] · Xian Liu[3] · Lijuan Wang[4] · Ping Chen[1] · Kun Nie[4] · Lixiang Chen[1] · Shuai Wang[1] · Biao Huang[2] · Ruiwang Huang[1]

Published online: 21 January 2019

Abstract

Freezing of gait (FOG), a disabling symptom of Parkinson's disease (PD), severely affects PD patients' life quality. Previous studies found neuropathologies in functional connectivity related to FOG, but few studies detected abnormal regional activities related to FOG in PD patients. In the present study, we analyzed the amplitude of low-frequency fluctuations (ALFF) to detect brain regions showing abnormal activity in PD patients with FOG (PD-with-FOG) and without FOG (PD-without-FOG). As different frequencies of neural oscillations in brain may reflect distinct brain functional and physiological properties, we conducted this study in three frequency bands, slow-5 (0.01–0.027 Hz), slow-4 (0.027–0.073 Hz), and classical frequency band (0.01–0.08 Hz). We acquired rs-fMRI data from 18 PD-with-FOG patients, 18 PD-without-FOG patients, and 17 healthy controls, then calculated voxel-wise ALFF across the whole brain and compared ALFF among the three groups in each frequency band. We found: (1) in slow-5, both PD-with-FOG and PD-without-FOG patients showed lower ALFF in the bilateral putamen compared to healthy controls, (2) in slow-4, PD-with-FOG patients showed higher ALFF in left inferior temporal gyrus (ITG) and lower ALFF in right middle frontal gyrus (MFG) compared to either PD-without-FOG patients or healthy controls, (3) in classical frequency band, PD-with-FOG patients also showed higher ALFF in ITG compared to either PD-without-FOG patients or healthy controls. Furthermore, we found that ALFF in MFG and ITG in slow-4 provided the highest classification accuracy (96.7%) in distinguishing PD-with-FOG from PD-without-FOG patients by using a stepwise multivariate pattern analysis. Our findings indicated frequency-specific regional spontaneous neural activity related to FOG, which may help to elucidate the pathogenesis of FOG.

Keywords Freezing of gait (FOG) · Amplitude of low-frequency fluctuations (ALFF) · Frequency band · Multivariate pattern analysis (MVPA) · Functional MRI

Huiqing Hu and Jingwu Chen contributed equally to this work.

✉ Biao Huang
cjr.huangbiao@vip.163.com

✉ Ruiwang Huang
ruiwang.huang@gmail.com

[1] Center for the Study of Applied Psychology, Key Laboratory of Mental Health and Cognitive Science of Guangdong Province, School of Psychology, South China Normal University, Guangzhou 510631, People's Republic of China

[2] Department of Radiology, Guangdong Academy of Medical Sciences, Guangdong General Hospital, Guangzhou 510030, People's Republic of China

[3] Department of Radiology, Guangdong Provincial Hospital of Chinese Medicine, Guangzhou 510030, People's Republic of China

[4] Department of Neurology, Guangdong General Hospital, Guangdong Academy of Medical Sciences, Guangzhou 510030, People's Republic of China

Introduction

Freezing of gait (FOG) is characterized by "brief, episodic absence or marked reduction of forward progression of the feet despite the intention to walk" (Giladi and Nieuwboer 2008). This impairment easily leads to fall and affects the life quality of patients with Parkinson's disease (PD) (Nonnekes et al. 2015). Although many debates about the pathogenesis of FOG (Nutt et al. 2011), we still do not have a clear understanding of it.

Previous neuroimaging studies (Lenka et al. 2016; Nutt et al. 2011) suggested that PD patients with FOG (PD-with-FOG) and without FOG (PD-without-FOG) may have both common and specific neuropathologies. In clinical situations, both PD-with-FOG and PD-

without-FOG patients have been observed motor and cognition declines, especially executive dysfunctions (Gratwicke et al. 2015; Snijders et al. 2016; Tahmasian et al. 2017). Neuroimaging studies on PD-with-FOG and PD-without-FOG have revealed their abnormal structure and function in the basal ganglia (BG), cerebellum (Canu et al. 2015; Esposito et al. 2013; Lewis and Shine 2016; Wu and Hallett 2013), and regions within the cognitive control, default mode (DMN), sensorimotor, and visual networks (Canu et al. 2015; Shine et al. 2013; Zhong et al. 2018). Actually, a sizable number of PD patients, about 20% - 50%, do not suffer from FOG in their life (Man et al. 2012).

Resting-state fMRI (rs-fMRI) has been applied to detect the underlying pathophysiology of FOG in PD patients (Canu et al. 2015; Lenka et al. 2016; Tessitore et al. 2012). Tessitore et al. (2012) found decreased functional connectivity (FC) within both the executive-attention (in the right middle frontal gyrus and in the angular gyrus) and visual networks (in the right occipito-temporal gyrus), and the abnormal FC within the two networks was correlated with the severity of FOG in PD patients. Lenka et al. (2016) found decreased FC within the primary somatosensory and auditory regions in PD-with-FOG patients compared to PD-without-FOG patients, and suggested that the decreased FC may reflect the impaired control and coordination of bilateral leg movements while walking. We noticed that these studies detected abnormal inter-regional temporal synchronization rather than regional spontaneous neural activity in PD-with-FOG patients. Although those studies can provide abnormal inter-regional FC, it is still hard to determine specific abnormal regions in PD-with-FOG patients.

The amplitude of low-frequency fluctuations (ALFF), obtained by calculating the square root of the power spectrum at each frequency and then averaging square root across a certain frequency band (Zang et al. 2007), can be used to describe the strength of regional spontaneous neural activity. For example, Zuo et al. (2010) found ALFF within gray matter was higher compared to ALFF within white matter. Kiviniemi et al. (2003) found higher ALFF in visual region than auditory and sensorimotor region.

In addition, ALFF may be a biomarker for physiological state of the brain. Yang et al. (2007) found ALFF in eyes-open condition was significantly higher than that in eyes-closed condition. Recently, ALFF has been applied to explore abnormal brain activity in various neurodegenerative diseases, such as Alzheimer's disease (AD) (Cai et al. 2016; Dai et al. 2012), PD (Caminiti et al. 2017; Skidmore et al. 2013), and amyotrophic lateral sclerosis (ALS) (Zhu et al. 2015). For example, previous studies (Li et al. 2017b; Mi et al. 2017; Skidmore et al. 2013) examined PD-related ALFF in the classical frequency band (0.01–0.08 Hz), and found abnormal ALFF in the basal ganglia, thalamus, and the prefrontal cortex; these regions are in line with findings in previous task-related (Cerasa et al. 2012; Michely et al. 2015) and structural neuroimaging (Li et al. 2017a) studies.

Buzsaki and Draguhn (2004) suggested different frequencies of neural oscillations in human brain may be sensitive to activity in different regions and can be used to reflect distinct physiological functions of brain activity. Previous studies (Biswal et al. 1995; Di Martino et al. 2008; Zuo et al. 2010) subdivided frequency spectrum into five different frequency bands, including slow-6 (0.0052–0.01 Hz), slow-5 (0.01–0.027 Hz), slow-4 (0.027–0.073 Hz), slow-3 (0.073–0.198 Hz) and slow-2 (0.198–0.25 Hz). The oscillations below 0.01 Hz can be considered to be scanner-related noise and thus can be removed or corrected (Fransson 2005). Further, oscillations were primarily detected within gray matter in slow-5 and slow-4, while in white matter signals in slow-3 and slow-2 (Salvador et al. 2008; Zuo et al. 2010). Thus, in the present study, we aimed to detect the altered ALFF in PD patients with and without freezing of gait in slow-5 and slow-4, but not in slow-6, slow-3 and slow-2. In fact, Zuo et al. (2010) found there were higher ALFF in the basal ganglia in slow-4 compared to slow-5, and higher ALFF in the ventromedial prefrontal cortex in slow-5 compared to in slow-4.

Several studies (Hou et al. 2014; Xue et al. 2016) showed that subdividing the classical frequency into slow-4 and slow-5 sub-bands was more sensitive to detect abnormal neural activity in brain disorder patients. For example, Xue et al. (2016) found that patients with major depressive disorder had lower regional homogeneity (ReHo) in the anterior cingulate cortex (ACC) and thalamus compared to healthy controls in slow-4 but not in the classical frequency band. The ACC and thalamus are believed to be associated with emotional processing and emotional control (Anand et al. 2005; Diener et al. 2012). Hou et al. (2014) found that PD patients showed abnormal ALFF in the brainstem and basal ganglia in both slow-4 and slow-5 sub-bands. We also noticed that several rs-fMRI studies (Choe et al. 2013; Kwak et al. 2012) failed to detect abnormal ALFF in the brainstem and basal ganglia in PD patients in classical frequency band, although most studies (Kalia and Lang 2015; Nutt et al. 2011) suggested that the brainstem and basal ganglia may be key regions in the pathophysiology of PD.

In the present study, our aim was to detect the altered regional spontaneous neural activity in both PD-with-FOG and PD-without-FOG patients. To this end, we acquired rs-fMRI data from 18 PD-with-FOG, 18 PD-without-FOG patients, and 17 healthy controls, estimated the voxel-wise ALFF across the whole brain, and compared the ALFF values among the three groups in each frequency band (classical frequency band, slow-4, and slow-5). Furthermore, we also conducted a stepwise multivariate pattern analysis (MVPA) to distinguish PD-with-FOG from PD-without-FOG patients separately for each of the three frequency bands.

Methods

Participants

Thirty-six levodopa-responsive patients with idiopathic PD, including 18 PD-with-FOG patients (12 M/6 F, aged 62.9 ± 10.7 years old), 18 PD-without-FOG patients (12 M/6 F, aged 61.3 ± 8.4 years old), and 17 healthy controls (11 M/6 F, aged 61.0 ± 8.0 years old), participated in the present study. All subjects were right-handed according to self-report. All the patients were diagnosed according to the clinical diagnostic criteria of the UK Parkinson's Disease Society Brain Bank (Hughes et al. 1992) by two experienced neurologists (W.L. and Z.Y.). Patients were classified as PD-with-FOG if they felt that their "feet get glued to the floor while walking, making a turn or when trying to initiate walking" (Giladi et al. 2000). For each patient, the severity of motor symptoms was assessed according to the Unified Parkinson's Disease Rating Scale (UPDRS-III) (Goetz 2003) and the stage of disease was determined based on the Hoehn and Yahr (H&Y) scale (Hoehn and Yahr 1998). All the subjects were screened for the presence of cognitive impairment using the Mini-Mental State Examination (MMSE) (Folstein et al. 1975). To minimize the impact of antiparkinsonian medication, we conducted the clinical evaluations and MRI scans at least 12 h after receiving dopaminergic medications ("OFF" state). The inclusion criteria for the patients were as follows: (a) diagnosis of idiopathic PD, (b) disease duration 1–15 years, and (c) Hoehn & Yahr stage ≤ 4 in the "OFF" state. The exclusion criteria for the patients were cognitive dysfunction (MMSE score < 24), or a history of neurological disorder or psychiatric illness or substance abuse or neuroanatomical abnormalities, or motor comorbidities. None of the healthy subjects had a history of neurological disorder, psychiatric illness, or any neuroanatomical abnormalities. At last, 4 patients (3 PD-with-FOG and 1 PD-without-FOG) were excluded because of MMSE score < 24. The study protocol was approved by the Institutional Review Board of the Guangdong General Hospital. Written informed consent was obtained from each subject prior to the study.

Data acquisition

All MRI data were obtained on a 3 T GE Signa Excite II HD MRI scanner equipped with an 8-channel phased-array head coil. The rs-fMRI data were acquired using a single-shot gradient-echo EPI sequence: repetition time (TR) = 2000 ms, echo time (TE) = 30 ms, flip angle = 80°, field of view (FOV) = 256 × 256 mm^2, matrix size = 64 × 64, in-plane resolution = 3.75 × 3.75 mm^2, slice thickness/gap = 4 mm/1 mm, 30 interleaved axial slices covering the whole-brain, and 186 volumes. During the scanning, the subjects were instructed to remain still, stay awake, close eyes, but not think about anything in particular. In addition, we also acquired high-resolution brain structural images by using a T1-weighted fast spoiled gradient recalled echo inversion recovery sequence: TR = 8.4 ms, TE = 3.3 ms, flip angle = 13°, FOV = 240 × 240 mm^2, matrix size = 256 × 256, slice thickness = 1 mm, voxel size = 0.94 × 0.94 × 1 mm^3, and 146 sagittal slices covering the whole-brain. Foam padding was used to minimize head motion and earplugs were adopted to reduce acoustic noise.

Data preprocessing

All the rs-fMRI data were processed using SPM12 (http://www.fil.ion.ucl.ac.uk/spm) and DPABI V2.3 (http://www.rfmri.org/dpabi). For each subject, we discarded the first 10 functional volumes to allow for adaptation to the environment and equilibrium of the MR signal and then retained the remaining 176 volumes for slice-timing correction and head-motion correction. In this study, we set the exclusion criteria for head motion as translation > 2 mm in any plane or rotation > 2° in any direction. Thus 4 patients' datasets (2 PD-with-FOG and 2 PD-without-FOG) were excluded, while no healthy controls dataset was abandoned because of head motion. The mean frame-wise displacement Jenkinson (FD-Jenkinson) (Jenkinson et al. 2002) was calculated for each subject. No significant difference in the mean FD-Jenkinson was found between the three groups (one-way ANOVA test, $p = 0.335$). Subsequently, the functional images were normalized to the MNI standard space by using the individual structural images and resampled to 3 × 3 × 3 mm^3. To remove the noise signal, we took the head motion (Friston-24 head motion parameters), signals of brain white matter (WM) and cerebrospinal fluid (CSF), whole-brain signal, and the linear drift as covariates and regressed them out. Finally, we retained 13 PD-with-FOG patients (9 M/4 F, aged 60.8 ± 11.9 years old), 15 PD-without-FOG patients (9 M/6 F, aged 60.9 ± 7.3 years old), and 17 healthy controls (11 M/6 F, aged 61.0 ± 8.0 years old) for further analyses. Table 1 lists the detailed information for all the subjects used in the further analyses.

ALFF calculation

The voxel-wise ALFF value was calculated for each subject using SPM12 and DPABI V2.3. We performed temporal band-pass filtering of the data in the three frequency bands. In the filtering procedure, the data were transformed from the time domain to the frequency domain, filtered, and then transformed back to the time domain. The filtered images were smoothed with a Gaussian kernel of 6 mm full-width-at-half-maximum (FWHM). In each frequency band, we first extracted the time course for each voxel and then converted it to the frequency domain using a fast Fourier transform (FFT). The

average square root of the power spectrum was computed in each frequency band and termed as ALFF (Zang et al. 2007). For standardization purposes, we divided the ALFF of each voxel by the whole-brain mean ALFF value.

Statistical analyses

One-way ANOVA was used to test between-group differences in age, education level, and MMSE score. Two-sample *t*-test was used to access the differences in UPDRS score and disease duration. In addition, χ^2-test was used to access differences in gender and H&Y score. Similar to previous studies (Aarsland et al. 2017; Ffytche et al. 2017), we found that both the PD-with-FOG and PD-without-FOG patients had significantly lower MMSE scores compared to the healthy controls. The present study therefore took the MMSE score as a covariate in the analyses.

One-way ANOVA was used to detect difference in ALFF among the three groups, the PD-with-FOG, PD-without-FOG patients, and healthy controls, in each frequency band, respectively. The multiple comparisons correction was performed using 3dClustSim (AFNI V16.2.11, https://afni.nimh.nih.gov/). The threshold was set at voxel level $p < 0.001$ and cluster level $p < 0.05$. In this way, we determined the clusters that had significant ALFF differences among the three groups. Subsequently, we saved those clusters as regions of interest (ROIs), and extracted the mean ALFF for each ROI. Then we performed two-sample *t*-tests to test the ALFF differences between each pair of groups in each frequency band ($p < 0.05$, FDR correction).

Stepwise multivariate pattern analyses

Using a stepwise multivariate pattern analyses (MVPA), we attempted to distinguish the PD-with-FOG patients from the PD-without-FOG patients based on the abnormal ALFF in different frequency bands, slow-4, slow-5, and the classical frequency band (Fig. 1). We selected the LIBSVM toolbox (http://www.csie.ntu.edu.tw/~cjlin/libsvm/) implemented in MATLAB and performed the following four steps. (1) Feature extraction: We used the clusters surviving from the one-way ANOVA in each frequency band as ROIs. For each patient, the mean ALFF for each ROI was extracted as a feature vector for the further stepwise classification. (2) Labelling: the PD-with-FOG patients were labeled as 1 and the PD-without-FOG patients were labeled as −1. (3) Determining classification weight: Using the feature vectors for all the patients, we applied a linear support vector machine (SVM) to perform the classifier training for slow-4, slow-5, and the classical frequency band, separately. This training model can be described by the following equation:

$$f(\mathrm{x}) = g(w_1 x_1 + \ldots w_i x_i), \quad (1)$$

where x_i and w_i represent the feature vector and the weight of the feature vector at the ROI *i*, respectively. The weight vector w_i is optimized such that the separating hyperplane defined by the prediction value $f(\mathrm{x})$ has the maximum margin. (4) Stepwise classification: Using sequential combinations of feature vectors, we conducted stepwise classifications in each frequency band. In this step, a SVM classifier was trained on the training samples and then applied to predict the class label for the testing sample. The "leave-one-out cross validation" (LOOCV) procedure (Pereira et al. 2009) was applied iteratively by leaving one subject out as the testing sample and taking the remaining subjects as training samples. We arranged all the features in the descending order of the classification weights, and sequentially added these features according to this order to train a model to conduct classification analyses. For example, given five features (A, B, C, D, and E), we first ranked them according to their classification weights in the descending order (e.g., B, A, D, E, C), and then

Table 1 Demographic and clinical information for the Parkinson's disease patients with freezing of gait (PD-with-FOG), the Parkinson's disease patients without freezing of gait (PD-without-FOG), and the healthy controls (HC)

	PD-with-FOG	PD-without-FOG	HC	$\chi^2/t/F$-value	*p* value
Gender (male/female)	9/4	9/6	11/6	0.260	0.878[a]
Age (years old)	60.8 ± 11.9	60.9 ± 7.3	61.0 ± 8.0	0.002	0.998[b]
Level of education (years)	9.9 ± 4.9	8.8 ± 2.3	9.7 ± 3.2	0.409	0.667[b]
UPDRS-III	36.5 ± 10.8	34.6 ± 9.2	–	0.485	0.632[c]
H&Y	2.9 ± 0.8	2.1 ± 0.6	–	8.185	0.146[a]
MMSE	26.6 ± 1.7	27.5 ± 1.6	28.9 ± 0.97	10.057	0.000[b]
Disease duration (years)	5.8 ± 4.0	4.3 ± 2.8	–	1.141	0.264[c]

UPDRS, the Unified Parkinson's Disease Rating scale; H&Y, Hoehn and Yahr scale; MMSE, Mini-Mental State Examination

[a] The *p* value was estimated using a two-tailed χ^2-test

[b] The *p* value was obtained from a one-way ANOVA

[c] The *p* value was obtained from a two-tailed dependent sample *t*-test

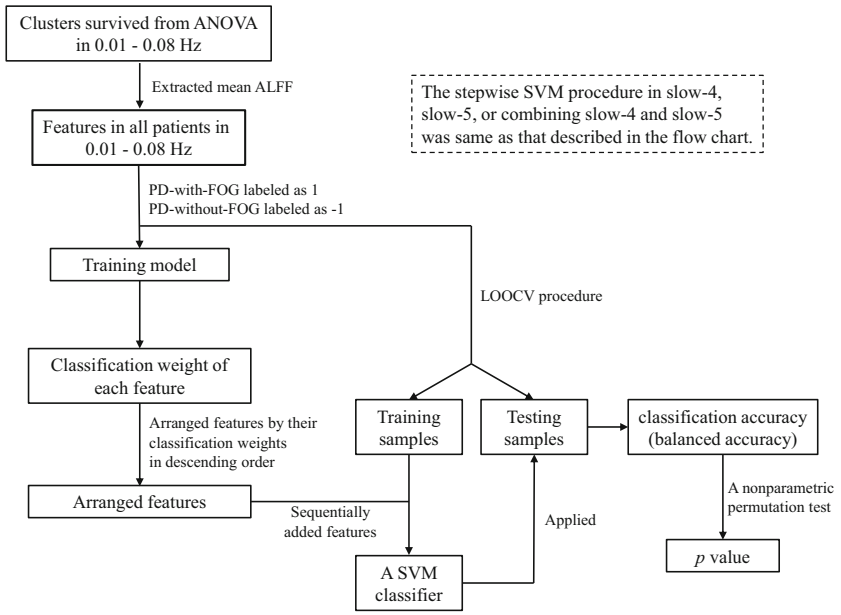

Fig. 1 The stepwise SVM procedure in classical frequency band (0.01–0.08 Hz), slow-4, slow-5, and the combination of slow-4 and slow-5

used the feature B to distinguish PD-with-FOG from PD-without-FOG patients. Afterward, we took the features B and A to distinguish PD-with-FOG from PD-without-FOG patients. Following this rule, we finally used all the five features to conduct the classification analysis. Since the number of subjects per group is not identical, we adopted the balanced accuracy (Brodersen et al. 2011) to represent the classification accuracy, which is given by:

$$\text{Balanced accuracy} = \frac{1}{2}\left(\frac{TP}{TP+FN}+\frac{TN}{TN+FP}\right), \qquad (2)$$

where TP, TN, FP and FN represent the number of true positives, true negatives, false positives, and false negatives, respectively. The sensitivity was estimated as the percentage of all the PD-with-FOG patients who were correctly identified as having FOG, TP / (TP + FN). The specificity was estimated as the percentage of PD-without-FOG patients who were correctly identified as not having FOG, TN / (TN + FP). The balanced accuracy is the averaged accuracy across the groups, (sensitivity + specificity) / 2.

Statistical significance of the classification accuracy was estimated using a nonparametric permutation test, in which different subjects and group labels were randomly associated with each other and then the classification analyses were conducted as described above. By repeating this random permutation procedure 5000 times, we determined the significance of the classification accuracy as the probability of its chance occurrence in these 5000 surrogate classifications. In addition, to determine whether classification accuracy obtained from a combination of features in slow-4 and slow-5 would higher than those obtained from each frequency band, we also used this combination of features to conduct a classification.

Results

Demographics and clinical characteristics

Table 1 lists the demographic and clinical characteristics of the PD-with-FOG, PD-without-FOG patients as well as the healthy controls. No significant difference was found in any of demographic variables, age ($F = 0.002$, $p = 0.998$), gender ($\chi^2 = 0.260$, $p = 0.878$), and level of education ($F = 0.409$, $p = 0.667$), across the three groups. No significant difference was found in disease duration ($t = 1.141$, $p = 0.264$), UPDRS-III ($t = 0.485$, $p = 0.632$), H&Y ($\chi^2 = 8.185$, $p = 0.146$) and MMSE scores (t = -1.342, $p = 0.191$) between the PD-with-FOG and PD-without-FOG patients. The healthy controls had a significantly higher MMSE score compared to either the PD-with-FOG (t = -4.397, p = 3.570e-4) or PD-without-FOG patients (t = -3.044, $p = 0.006$).

ALFF analyses

Figure 2 shows the clusters with significant difference in ALFF among the three groups, the PD-with-FOG patients, PD-without-FOG patients, and healthy controls. In the classical frequency band, we found significantly different ALFF among the three groups in three clusters, 2 in the left inferior temporal gyrus (ITG) and 1 in the left middle temporal gyrus (MTG). In slow-4, we found significantly different ALFF among the three groups in two clusters, which are located in the left ITG and right middle frontal gyrus (MFG). In slow-5, we found significantly different ALFF among the three groups in two clusters, which are located in the bilateral putamen. The detailed information for these clusters is listed in Table 2.

The clusters with significant difference in ALFF were also determined for each pair of groups. In the classical frequency

band, the PD-with-FOG patients had significantly higher ALFF in the left ITG and left MTG compared to either the PD-without-FOG patients or healthy controls. In slow-4, the PD-with-FOG patients had significantly higher ALFF in the left ITG and lower ALFF in the right MFG compared to either the PD-without-FOG patients or healthy controls. The PD-without-FOG patients had significantly higher ALFF in the right MFG and lower ALFF in the left ITG compared to the healthy controls. In slow-5, both the PD-with-FOG and PD-without-FOG patients had significantly lower ALFF in the bilateral putamen compared to the healthy controls.

Stepwise multivariate pattern analyses

Figure 3 and Table 3 illustrate the classification performance of using features in the classical frequency, slow-4, and slow-5 as well as the combination of the two frequency sub-bands to differentiate the PD-with-FOG from the PD-without-FOG patients. In classical frequency band, the highest classification weight corresponds to ALFF in the left ITG. In slow-4, the highest classification weight corresponds to ALFF in the right MFG. In slow-5, the highest classification weight corresponds to ALFF in the left putamen. When combined features in slow-4 and slow-5 to conduct the classification, the highest classification weight corresponds to ALFF in the right MFG in slow-4. In the classical frequency band, the ALFF values in the left ITG and left MTG provided a classification accuracy of 92.8% ($p < 0.001$). In slow-4, the highest classification accuracy, provided by the ALFF values in the right MFG and left ITG, was 96.7% ($p < 0.001$). In slow-5, the ALFF values in the left putamen provided a classification accuracy of 41.0% ($p = 0.834$). When we combined features in the slow-4 and slow-5, we obtained the highest accuracy of 96.7% ($p < 0.001$) by the ALFF values in the right MFG and left ITG in the slow-4 (Fig. 3d).

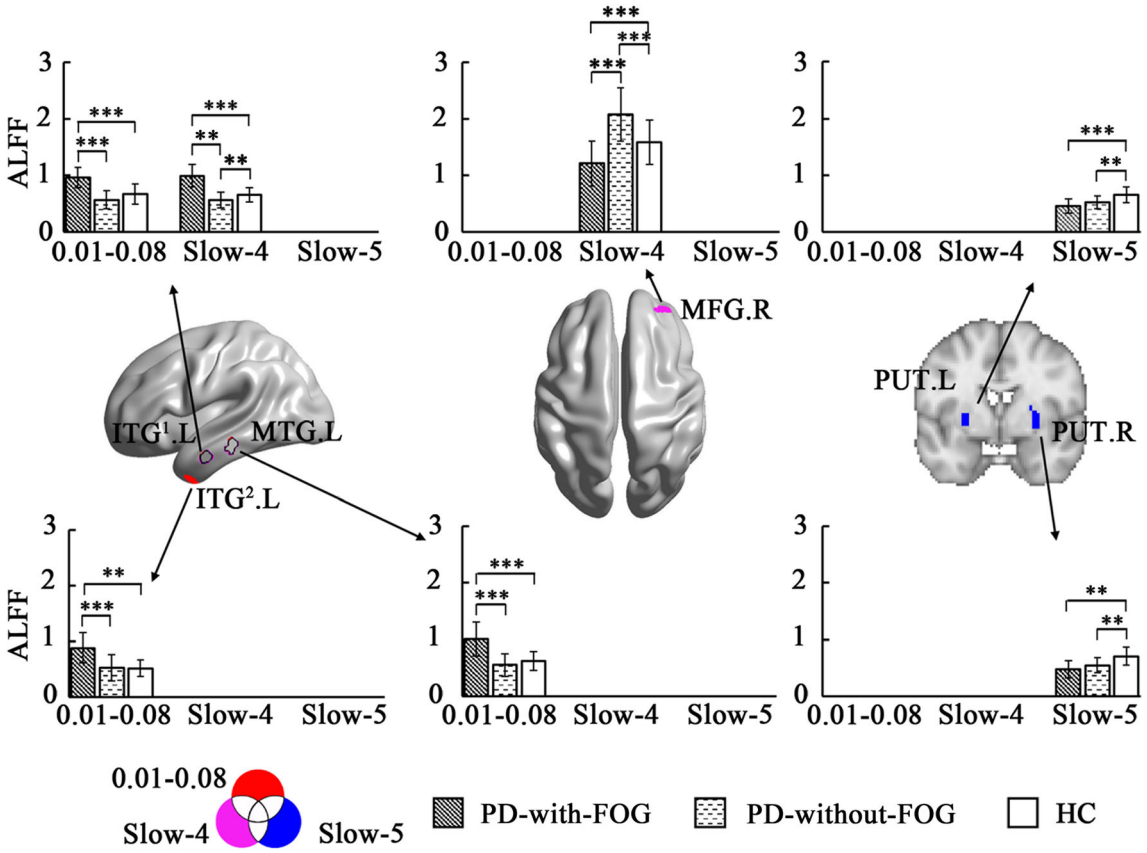

Fig. 2 Spatial location of the clusters with significant group differences in the amplitude of low frequency fluctuations (ALFF) levels between the three groups, PD patients with freezing of gait (PD-with-FOG), PD patients without freezing of gait (PD-without-FOG), and healthy controls (HC) in three frequency bands. The clusters color-coded in red, purple, and blue indicate clusters with significant group differences in ALFF levels specific to, respectively, the classical frequency (0.01–0.08 Hz), slow-4 (0.027–0.073 Hz), and slow-5 (0.01–0.027 Hz) bands. The clusters color-contoured in black indicate the intersection clusters, in which the ALFF levels showed significant group differences in any two of the three frequency bands. These clusters were determined using 3dClustSim correction (voxel level $p < 0.001$ and cluster level $p < 0.05$) and post-hoc analyses ($p < 0.05$, FDR-corrected). The images are presented according to neurological convention. The bars and error bars correspond to the average ALFF and the standard deviation for a given subject group of PD-with-FOG, or PD-without-FOG, or HC. ITG[1].L ($x = -60$, $y = -9$, $z = -24$); ITG[2].L ($x = -42$, $y = 3$, $z = -42$); L (R), left (right) hemisphere; ***, $p < 0.001$ and ** $p < 0.01$

Table 2 Clusters with significant difference in the mean amplitude of low frequency fluctuations (ALFF) across the three groups: Parkinson's disease patients with freezing of gait (PD-with-FOG), Parkinson's disease patients without freezing of gait (PD-without-FOG), and healthy controls (HC), in three frequency bands (One-way ANOVA, 3dClustSim correction with voxel level $p < 0.001$ and cluster level $p < 0.05$)

Clusters		BA	Peak coordinates in MNI space			Cluster size (# *voxels*)	*F*-value
			x	*y*	*z*		
0.01–0.08 Hz							
ITG.L	PD-with-FOG > PD- without-FOG = HC	21	−60	−9	−24	20	20.83
ITG.L	PD-with-FOG > PD-without-FOG = HC	20	−42	3	−42	21	16.31
MTG.L	PD-with-FOG > PD-without-FOG = HC	20	−63	−27	−15	21	13.26
Slow-4 (0.027–0.073 Hz)							
ITG.L	PD-with-FOG > HC > PD-without-FOG	21	−60	−9	−24	43	18.37
MFG.R	PD-without-FOG > HC > PD-with-FOG	46	33	54	18	19	15.24
Slow-5 (0.01–0.027 Hz)							
PUT.L	HC > PD-without-FOG = PD-with-FOG	48	−24	6	−3	19	13.39
PUT.R	HC > PD-without-FOG = PD-with-FOG	48	27	0	−3	18	11.31

ITG, inferior temporal gyrus; MTG, middle temporal gyrus; MFG, middle frontal gyrus; PUT, putamen; BA, Brodmann's areas; L (R), left (right) hemisphere. # number of voxels in clusters; = indicates there was no significant difference in ALFF between the two groups

Discussion

In the present study, we examined altered ALFF in the PD-with-FOG and PD-without-FOG patients in slow-4, slow-5, and classical frequency band separately. Furthermore, using a stepwise MVPA, we identified several brain regions whose ALFF values could be used to differentiate the PD-with-FOG from PD-without-FOG patients. We obtained the following results: i) Both the PD-with-FOG and PD-without-FOG patients had lower ALFF in bilateral putamen. ii) The PD-with-FOG patients had specific higher ALFF in the left ITG and left MTG, and lower ALFF in the right MFG, compared with either the PD-without-FOG patients or healthy controls. iii) The abnormal ALFF in the putamen in the PD-with-FOG and PD-without-FOG patients was in slow-5, but neither in slow-4 nor in the classical frequency band. iv) The ALFF values in the MFG and ITG in slow-4 were important in distinguishing the PD-with-FOG from the PD-without-FOG patients.

Common altered ALFF in both PD-with-FOG and PD-without-FOG patients

Both the PD-with-FOG and PD-without-FOG patients showed significant lower ALFF in the bilateral putamen

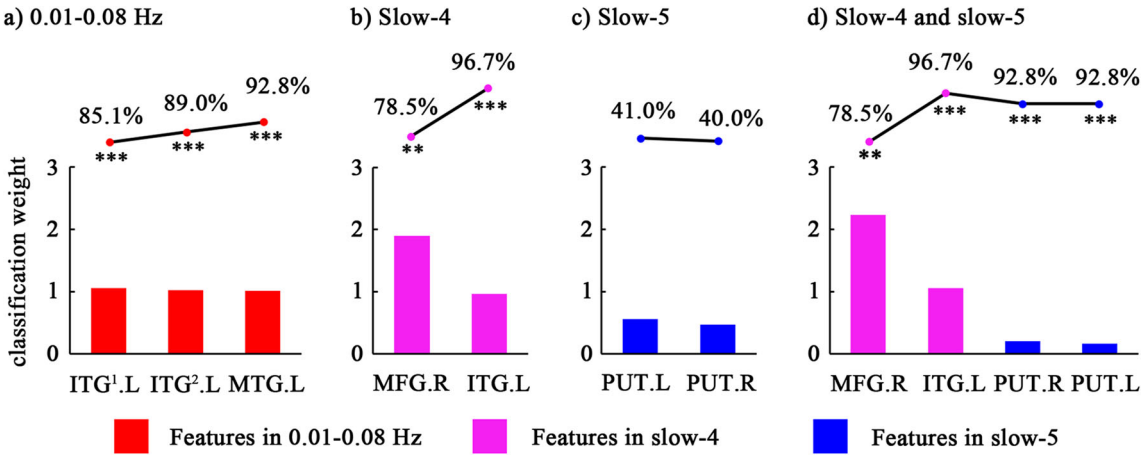

Fig. 3 Stepwise classification of the PD patients with freezing of gait (PD-with-FOG) from the PD patients without freezing of gait (PD-without-FOG) in different frequency bands based on ALFF. **a** Classical frequency band (0.01–0.08 Hz), (**b**) Slow-4 (0.027–0.073 Hz), (**c**) Slow-5 (0.01–0.027 Hz), and (**d**) Two frequency sub-bands (slow-4 and slow-5). The histogram shows the classification weight of each feature in the classification analyses. All the feature were arranged in descending order based on their classification weight. During stepwise classification analysis, we sequential combined the features to differentiate the PD-with-FOG from the PD-without-FOG patients according to the rank of features' classification weights. The line above histogram shows the accuracy of the stepwise classification for each frequency band. ITG[1].L ($x = -60, y = -9, z = -24$); ITG[2].L ($x = -42, y = 3, z = -42$). ***, $p < 0.001$ and **, $p < 0.01$

Table 3 Performance of differentiating the PD patients with freezing of gait (PD-with-FOG) from the PD patients without freezing of gait (PD-without-FOG) in different frequency bands using ALFF. Balanced accuracy was given in eq.2

Frequency band	Sensitivity	Specificity	Balanced accuracy	*p* value
0.01–0.08 Hz	92.3%	93.3%	92.8%	< 0.001
Slow-4 (0.027-0.073 Hz)	100.0%	93.3%	96.7%	< 0.001
Slow-5 (0.01-0.027 Hz)	0.0%	80.0%	40.0%	0.834
Slow-4 and slow-5	92.3%	93.3%	92.8%	< 0.001

compared to the healthy controls (Table 2). This result was partially consistent with previous studies (Chen et al. 2015; Hou et al. 2014; Mi et al. 2017; Pan et al. 2017). Several studies (Goldstein et al. 2017; Kish et al. 2017) have reported dopamine deficiency in the striatum in PD patients and found that the most severely affected region was the putamen. The putamen was suggested to be involved in self-initiated movement (Kamei 2013) and its dysfunction was shown to relate to clinical symptoms, such as bradykinesia, in PD patients (Prodoehl et al. 2010; Rodriguez-Oroz et al. 2009). For example, Prodoehl et al. (2010) performed a fMRI study with precision grip force task and found that PD patients had significant lower activation in putamen and the activation was negatively correlated with score of bradykinesia. Some studies found ALFF in the putamen was negatively correlated with disease duration and UPDRS score (Hou et al. 2014), and H&Y stage (Chen et al. 2015) in PD patients. The present study found no significant difference in ALFF in the putamen between the PD-with-FOG and the PD-without-FOG patients. This result is consistent with a previous study (Mi et al. 2017), which also found significant lower ALFF in the putamen in the PD-with-FOG and PD-without-FOG patients compared to healthy control, and did not find significantly different ALFF in this region between the PD-with-FOG and PD-without-FOG patients. Thus the lower ALFF in the putamen is likely a reflection of dysfunction in this region in patients with PD.

Specific altered ALFF in either PD-with-FOG or PD-without-FOG patients

In this study, we found significant higher ALFF in the left ITG (BA 20) and left MTG (BA 21) in the PD-with-FOG patients compared to either the PD-without-FOG patients or the healthy controls (Fig. 2). The anterior ITG and MTG are thought to be involved in multimodal semantic processing (Jackson et al. 2018; Visser et al. 2012). Ricciardi et al. (2014) found that PD-with-FOG patients performed worse in tasks of phonological verbal fluency compared to PD-without-FOG patients. They also found significant negative correlation between FOG severity (determined by FOG-Q) and phonological fluency in PD-with-FOG patients. In the present study, we found significant higher ALFF in both the anterior ITG and MTG in the PD-with-FOG patients compared to either the PD-without-FOG patients or healthy controls. This finding may indicate abnormal semantic processing in PD-with-FOG patients. Actually, no study has provided direct evidence on the relationship between brain activity in either ITG or MTG and semantic processing in PD-with-FOG patients.

In the right MFG (BA 46), we found that the PD-with-FOG patients had significant lower ALFF compared to the PD-without-FOG patients or healthy controls, while the PD-without-FOG patients had higher ALFF compared to the healthy controls (Table 2). This result is partly consistent with previous studies (Mi et al. 2017; Vercruysse et al. 2014). The MFG is believed to be responsible for executive functions, such as planning (Nitschke et al. 2017) and working memory (Curtis 2006). Actually, FOG is no longer considered as a pure motor impairment; the cognitive factors such as set-shifting (Naismith et al. 2010) and conflict resolution (Vandenbossche et al. 2011) have been suggested to be a cause of FOG. Previous studies found that PD-with-FOG patients had worse performance during an auditory version of the Stroop task (Vervoort et al. 2016) and Trail Making Test (Naismith et al. 2010) compared to PD-without-FOG, which revealed more severe deficit executive function in PD-with-FOG patients. Moreover, Mi et al. (2017) detected a negative correlation between ALFF in the prefrontal cortex and executive function sub-score (a part of Montreal Cognitive Assessment scale). Thus, the lower ALFF in the MFG may reflect a more severe interrupted executive function in the PD-with-FOG patients. In addition, we found that the PD-without-FOG patients had significant higher ALFF in the MFG compared to healthy controls. Lee et al. (2014) found that applying high frequency transcranial magnetic stimulation (TMS), which can increase region's activation (Lefaucheur et al. 2014), over the DLPFC could significantly reduce the UPDRS-III score and improve PD patients' locomotor performance. Thus we suggested that the higher ALFF in MFG may reflect a compensatory mechanism in PD-without-FOG patients.

We calculated ALFF in PD patients in different sub-band (slow-4 and slow-5). This is an efficient way to detect abnormal regional properties of spontaneous brain activity in PD patients. In the present study, we detected abnormal ALFF in the putamen in slow-5 but not in the classical frequency band.

We also found abnormal ALFF in the right MFG in slow-4 but not in the classical frequency band. Many studies (Buzsaki and Draguhn 2004; Xue et al. 2016; Zuo et al. 2010) suggested that neural activity in different regions can be sensitively detected in different frequency bands. Therefore, simply detecting brain activity in the classical frequency band may risk overlooking meaningful information from frequency-specific spontaneous BOLD fluctuations.

Stepwise multivariate pattern analyses

The ALFF pattern in the MFG and ITG can be used to distinguish PD-with-FOG patients from PD-without-FOG patients. With the application of MVPA, we found that ALFF value in the bilateral putamen in slow-5 only provided a classification accuracy of 40% in differentiating the PD-with-FOG patients from the PD-without-FOG patients. When combining ALFF in the bilateral putamen in slow-5 and ALFF value in the right MFG and left ITG in slow-4 together, we found that the classification accuracy increased to 92.8%. Furthermore, we obtained the highest classification accuracy (96.7%) in differentiating the PD-with-FOG patients from the PD-without-FOG patients by using ALFF in the right MFG and left ITG in slow-4. Previous studies (Moore et al. 2013; Zach et al. 2015) reported the classification of PD-with-FOG patients from PD-without-FOG patients based on behavioral data, such as the absolute number and duration of FOG events, and found the classification accuracy was less than 85%. This classification accuracy in the present study was higher than those of previous studies. The high classification provided by ALFF in the ITG and MFG in slow-4 showed that ALFF patterns in the ITG and MFG in slow-4 may have great difference between the PD-with-FOG and PD-without-FOG patients. Considering that the anterior ITG is involved in multimodal semantic processing (Jackson et al. 2018; Visser et al. 2012) and MFG is responsible for executive functions (Nitschke et al. 2017), we suggested that there may be different semantic processing function and executive function in PD-with-FOG and PD-without-FOG patients (Ricciardi et al. 2014; Vervoort et al. 2016).

Limitations

This study had several limitations. First, the small sample size of patients may limit the generality of the findings and may reduce statistical power for detecting group differences. Second, the PD-with-FOG patients and PD-without-FOG patients had significant lower MMSE scores compared to the healthy controls. This may bias our findings, although we took the group difference in MMSE score as a covariate. The significant lower MMSE scores in the PD-with-FOG and PD-without-FOG patients may suggest cognitive deficits in the two groups. Thus the abnormal ALFF in the MFG, ITG and MTG in the PD-with-FOG or PD-without-FOG patients observed in the present study should be carefully interpreted. Third, the FOG questionnaire score of each PD-with-FOG patient was not evaluated. Thus, we could not estimate the correlation between the ALFF and the severity of FOG for the detected abnormal region. Fourth, the result of rs-fMRI analysis may be contaminated by the cerebrovascular reactivity (CVR), which was not measured in this study. As BOLD-fMRI signal based on vascular responses secondary to neural activity (Ogawa and Lee 1990), the altered fMRI signal may be partly from a vascular change (Birn et al. 2008; van Buuren et al. 2009).

In summary, we detected the common and specific brain regions with altered amplitude of low-frequency fluctuations in PD-with-FOG and PD-without-FOG patients in different frequency bands. Both the PD-with-FOG and PD-without-FOG patients had common disruptions in regions related to motor functions. Specifically, the PD-with-FOG patients had disruption in regions related to semantic processing and executive function. Additionally, ALFF value of the MFG and ITG in slow-4 provided the highest accuracy in differentiating the PD-with-FOG from PD-without-FOG patients using MVPA. Our findings may be helpful for further revealing the frequency-dependent neural mechanisms in PD patients, either with or without FOG.

Acknowledgments The study was supported by grants from the National Natural Science Foundation of China [Grant numbers: 81871338, 81471654, 81428013, 81671275, and 81371535]; Planned Science and Technology Project of Guangdong Province, China [Grant numbers: 2014B020212022, 1563000653, 20160402007]; Innovation Project of Graduate School of South China Normal University. The funding organizations played no further role in study design, data collection, analysis and interpretation, and paper writing. The authors appreciate the editing assistance of Drs.Rhoda E. and Edmund F. Perozzi.

Compliance with ethical standards

Conflict of interest The authors declare that they have no conflict of interest.

Informed consent All procedures followed were in accordance with the ethical standards of the responsible committee on human experimentation (institutional and national) and with the Helsinki Declaration of 1975, as revised in 2000. Informed consent was obtained from all participants for being included in the study.

References

Aarsland, D., Creese, B., Politis, M., Chaudhuri, K. R., Ffytche, D. H., Weintraub, D., & Ballard, C. (2017). Cognitive decline in Parkinson disease. *Nature Reviews. Neurology, 13*(4), 217–231. https://doi.org/10.1038/nrneurol.2017.27.

Anand, A., Li, Y., Wang, Y., Wu, J., Gao, S., Bukhari, L., Mathews, V. P., Kalnin, A., & Lowe, M. J. (2005). Activity and connectivity of brain mood regulating circuit in depression: A functional magnetic resonance study. *Biological Psychiatry, 57*(10), 1079–1088. https://doi.org/10.1016/j.biopsych.2005.02.021.

Birn, R. M., Murphy, K., & Bandettini, P. A. (2008). The effect of respiration variations on independent component analysis results of resting state functional connectivity. *Human Brain Mapping, 29*(7), 740–750. https://doi.org/10.1002/hbm.20577.

Biswal, B., Yetkin, F. Z., Haughton, V. M., & Hyde, J. S. (1995). Functional connectivity in the motor cortex of resting human brain using echo-planar MRI. *Magnetic Resonance in Medicine, 34*(4), 537–541. https://doi.org/10.1002/mrm.1910340409.

Brodersen, K. H., Schofield, T. M., Leff, A. P., Ong, C. S., Lomakina, E. I., Buhmann, J. M., & Stephan, K. E. (2011). Generative embedding for model-based classification of fMRI data. *PLoS Computational Biology, 7*(6), e1002079. https://doi.org/10.1371/journal.pcbi.1002079.

Buzsaki, G., & Draguhn, A. (2004). Neuronal oscillations in cortical networks. *Science, 304*(5679), 1926–1929. https://doi.org/10.1126/science.1099745.

Cai, S., Tao, C., Peng, Y., Shen, W., Li, J., Deneen, K. M. V., & Huang, L. (2016). Altered functional brain networks in amnestic mild cognitive impairment: A resting-state fMRI study. *Brain Imaging and Behavior, 11*(3), 619–631. https://doi.org/10.1007/s11682-016-9539-0.

Caminiti, S. P., Presotto, L., Baroncini, D., Garibotto, V., Moresco, R. M., Gianolli, L., Volonté, M. A., Antonini, A., & Perani, D. (2017). Axonal damage and loss of connectivity in nigrostriatal and mesolimbic dopamine pathways in early Parkinson's disease. *Neuroimage Clin, 14*(C), 734–740. https://doi.org/10.1016/j.nicl.2017.03.011.

Canu, E., Agosta, F., Sarasso, E., Volonte, M. A., Basaia, S., Stojkovic, T., Stefanova, E., Comi, G., Falini, A., Kostic, V. S., Gatti, R., & Filippi, M. (2015). Brain structural and functional connectivity in Parkinson's disease with freezing of gait. *Human Brain Mapping, 36*(12), 5064–5078. https://doi.org/10.1002/hbm.22994.

Cerasa, A., Pugliese, P., Messina, D., Morelli, M., Gioia, M. C., Salsone, M., Novellino, F., Nicoletti, G., Arabia, G., & Quattrone, A. (2012). Prefrontal alterations in Parkinson's disease with levodopa-induced dyskinesia during fMRI motor task. *Movement Disorders, 27*(3), 364–371. https://doi.org/10.1002/mds.24017.

Chen, H. M., Wang, Z. J., Fang, J. P., Gao, L. Y., Ma, L. Y., Wu, T., Hou, Y. N., Zhang, J. R., & Feng, T. (2015). Different patterns of spontaneous brain activity between tremor-dominant and postural instability/gait difficulty subtypes of Parkinson's disease: A resting-state fMRI study. *CNS Neuroscience & Therapeutics, 21*(10), 855–866. https://doi.org/10.1111/cns.12464.

Choe, I. H., Yeo, S., Chung, K. C., Kim, S. H., & Lim, S. (2013). Decreased and increased cerebral regional homogeneity in early Parkinson's disease. *Brain Research, 1527*, 230–237. https://doi.org/10.1016/j.brainres.2013.06.027.

Curtis, C. E. (2006). Prefrontal and parietal contributions to spatial working memory. *Neuroscience, 139*(1), 173–180. https://doi.org/10.1016/j.neuroscience.2005.04.070.

Dai, Z., Yan, C., Wang, Z., Wang, J., Xia, M., Li, K., & He, Y. (2012). Discriminative analysis of early Alzheimer's disease using multimodal imaging and multi-level characterization with multi-classifier (M3). *Neuroimage, 59*(3), 2187–2195. https://doi.org/10.1016/j.neuroimage.2011.10.003.

Di Martino, A., Ghaffari, M., Curchack, J., Reiss, P., Hyde, C., Vannucci, M., Petkova, E., Klein, D. F., & Castellanos, F. X. (2008). Decomposing intra-subject variability in children with attention-deficit/hyperactivity disorder. *Biological Psychiatry, 64*(7), 607–614. https://doi.org/10.1016/j.biopsych.2008.03.008.

Diener, C., Kuehner, C., Brusniak, W., Ubl, B., Wessa, M., & Flor, H. (2012). A meta-analysis of neurofunctional imaging studies of emotion and cognition in major depression. *Neuroimage, 61*(3), 677–685. https://doi.org/10.1016/j.neuroimage.2012.04.005.

Esposito, F., Tessitore, A., Giordano, A., De Micco, R., Paccone, A., Conforti, R., Pignataro, G., Annunziato, L., & Tedeschi, G. (2013). Rhythm-specific modulation of the sensorimotor network in drug-naive patients with Parkinson's disease by levodopa. *Brain, 136*(Pt 3), 710–725. https://doi.org/10.1093/brain/awt007.

Ffytche, D. H., Creese, B., Politis, M., Chaudhuri, K. R., Weintraub, D., Ballard, C., & Aarsland, D. (2017). The psychosis spectrum in Parkinson disease. *Nature Reviews. Neurology, 13*(2), 81–95. https://doi.org/10.1038/nrneurol.2016.200.

Folstein, M. F., Folstein, S. E., & McHugh, P. R. (1975). Mini-mental state. A practical method for grading the cognitive state of patients for the clinician. *Journal of Psychiatric Research, 12*(3), 189–198. https://doi.org/10.1016/0022-3956(75)90026-6.

Fransson, P. (2005). Spontaneous low-frequency BOLD signal fluctuations: An fMRI investigation of the resting-state default mode of brain function hypothesis. *Human Brain Mapping, 26*(1), 15–29. https://doi.org/10.1002/hbm.20113.

Giladi, N., & Nieuwboer, A. (2008). Understanding and treating freezing of gait in parkinsonism, proposed working definition, and setting the stage. *Movement Disorders, 23*(Suppl 2), S423–S425. https://doi.org/10.1002/mds.21927.

Giladi, N., Shabtai, H., Simon, E. S., Biran, S., Tal, J., & Korczyn, A. D. (2000). Construction of freezing of gait questionnaire for patients with parkinsonism. *Parkinsonism & Related Disorders, 6*(3), 165–170. https://doi.org/10.1016/S1353-8020(99)00062-0.

Goetz, C. G. (2003). The unified Parkinson's disease rating scale (UPDRS): Status and recommendations. *Movement Disorders, 18*(7), 738–750. https://doi.org/10.1002/mds.10473.

Goldstein, D. S., Sullivan, P., Holmes, C., Mash, D. C., Kopin, I. J., & Sharabi, Y. (2017). Determinants of denervation-independent depletion of putamen dopamine in Parkinson's disease and multiple system atrophy. *Parkinsonism & Related Disorders, 35*, 88–91. https://doi.org/10.1016/j.parkreldis.2016.12.011.

Gratwicke, J., Jahanshahi, M., & Foltynie, T. (2015). Parkinson's disease dementia: A neural networks perspective. *Brain, 138*(6), 1454–1476. https://doi.org/10.1093/brain/awv104.

Hoehn, M. M., & Yahr, M. D. (1998). Parkinsonism: onset, progression, and mortality. *Neurology, 50*(2), 11–26. https://doi.org/10.1212/WNL.17.5.427.

Hou, Y., Wu, X., Hallett, M., Chan, P., & Wu, T. (2014). Frequency-dependent neural activity in Parkinson's disease. *Human Brain Mapping, 35*(12), 5815–5833. https://doi.org/10.1002/hbm.22587.

Hughes, A. J., Daniel, S. E., Kilford, L., & Lees, A. J. (1992). Accuracy of clinical diagnosis of idiopathic Parkinson's disease: A clinico-pathological study of 100 cases. *Journal of Neurology, Neurosurgery, and Psychiatry, 55*(3), 181–184. https://doi.org/10.1136/jnnp.55.3.181.

Jackson, R. L., Bajada, C. J., Rice, G. E., Cloutman, L. L., & Lambon Ralph, M. A. (2018). An emergent functional parcellation of the temporal cortex. *Neuroimage, 170*, 385–399. https://doi.org/10.1016/j.neuroimage.2017.04.024.

Jenkinson, M., Bannister, P., Brady, M., & Smith, S. (2002). Improved optimization for the robust and accurate linear registration and motion correction of brain images. *Neuroimage, 17*(2), 825–841. https://doi.org/10.1006/nimg.2002.1132.

Kalia, L. V., & Lang, A. E. (2015). Parkinson's disease. *Lancet, 386*(9996), 896–912. https://doi.org/10.1016/s0140-6736(14)61393-3.

Kamei, S. (2013). Executive dysfunction in Parkinson's disease: A review. *Journal of Neuropsychology, 7*(2), 193–224. https://doi.org/10.1111/jnp.12028.

Kish, S. J., Boileau, I., Callaghan, R. C., & Tong, J. (2017). Brain dopamine neurone 'damage': Methamphetamine users vs. Parkinson's disease - a critical assessment of the evidence. *The European Journal of Neuroscience, 45*(1), 58–66. https://doi.org/10.1111/ejn.13363.

Kiviniemi, V., Kantola, J. H., Jauhiainen, J., Hyvarinen, A., & Tervonen, O. (2003). Independent component analysis of nondeterministic fMRI signal sources. *Neuroimage, 19*(2 Pt 1), 253–260. https://doi.org/10.1016/S1053-8119(03)00097-1.

Kwak, Y., Peltier, S. J., Bohnen, N. I., Muller, M. L., Dayalu, P., & Seidler, R. D. (2012). L-DOPA changes spontaneous low-frequency BOLD signal oscillations in Parkinson's disease: A resting state fMRI study. *Frontiers in Systems Neuroscience, 6*(6), 52. https://doi.org/10.3389/fnsys.2012.00052.

Lee, S. Y., Kim, M. S., Chang, W. H., Cho, J. W., Youn, J. Y., & Kim, Y. H. (2014). Effects of repetitive transcranial magnetic stimulation on freezing of gait in patients with parkinsonism. *Restorative Neurology and Neuroscience, 32*(6), 743–753. https://doi.org/10.3233/rnn-140397.

Lefaucheur, J. P., Andre-Obadia, N., Antal, A., Ayache, S. S., Baeken, C., Benninger, D. H., Cantello, R. M., Cincotta, M., de Carvalho, M., De Ridder, D., Devanne, H., Di Lazzaro, V., Filipovic, S. R., Hummel, F. C., Jaaskelainen, S. K., Kimiskidis, V. K., Koch, G., Langguth, B., Nyffeler, T., Oliviero, A., Padberg, F., Poulet, E., Rossi, S., Rossini, P. M., Rothwell, J. C., Schonfeldt-Lecuona, C., Siebner, H. R., Slotema, C. W., Stagg, C. J., Valls-Sole, J., Ziemann, U., Paulus, W., & Garcia-Larrea, L. (2014). Evidence-based guidelines on the therapeutic use of repetitive transcranial magnetic stimulation (rTMS). *Clinical Neurophysiology, 125*(11), 2150–2206. https://doi.org/10.1016/j.clinph.2014.05.021.

Lenka, A., Naduthota, R. M., Jha, M., Panda, R., Prajapati, A., Jhunjhunwala, K., Saini, J., Yadav, R., Bharath, R. D., & Pal, P. K. (2016). Freezing of gait in Parkinson's disease is associated with altered functional brain connectivity. *Parkinsonism & Related Disorders, 24*, 100–106. https://doi.org/10.1016/j.parkreldis.2015.12.016.

Lewis, S. J., & Shine, J. M. (2016). The next step: A common neural mechanism for freezing of gait. *Neuroscientist, 22*(1), 72–82. https://doi.org/10.1177/1073858414559101.

Li, C., Huang, B., Zhang, R., Ma, Q., Yang, W., Wang, L., Wang, L., Xu, Q., Feng, J., Liu, L., Zhang, Y., & Huang, R. (2017a). Impaired topological architecture of brain structural networks in idiopathic Parkinson's disease: A DTI study. *Brain Imaging and Behavior, 11*(1), 113–128. https://doi.org/10.1007/s11682-015-9501-6.

Li, D., Huang, P., Zang, Y., Lou, Y., Cen, Z., Gu, Q., Xuan, M., Xie, F., Ouyang, Z., Wang, B., Zhang, M., & Luo, W. (2017b). Abnormal baseline brain activity in Parkinson's disease with and without REM sleep behavior disorder: A resting-state functional MRI study. *Journal of Magnetic Resonance Imaging, 46*(3), 697–703. https://doi.org/10.1002/jmri.25571.

Man, A., Tsoi, T. H., Mok, V., Cheung, C. M., Lee, C. N., Li, R., & Yeung, E. (2012). Ten year survival and outcomes in a prospective cohort of new onset Chinese Parkinson's disease patients. *Journal of Neurology, Neurosurgery, and Psychiatry, 83*(6), 607–611. https://doi.org/10.1136/jnnp-2011-301590.

Mi, T. M., Mei, S. S., Liang, P. P., Gao, L. L., Li, K. C., Wu, T., & Chan, P. (2017). Altered resting-state brain activity in Parkinson's disease patients with freezing of gait. *Scientific Reports, 7*(1), 16711. https://doi.org/10.1038/s41598-017-16922-0.

Michely, J., Volz, L. J., Barbe, M. T., Hoffstaedter, F., Viswanathan, S., Timmermann, L., Eickhoff, S. B., Fink, G. R., & Grefkes, C. (2015). Dopaminergic modulation of motor network dynamics in Parkinson's disease. *Brain, 138*(Pt 3), 664–678. https://doi.org/10.1093/brain/awu381.

Moore, S. T., Yungher, D. A., Morris, T. R., Dilda, V., MacDougall, H. G., Shine, J. M., Naismith, S. L., & Lewis, S. J. (2013). Autonomous identification of freezing of gait in Parkinson's disease from lower-body segmental accelerometry. *Journal of Neuroengineering and Rehabilitation, 10*, 19. https://doi.org/10.1186/1743-0003-10-19.

Naismith, S. L., Shine, J. M., & Lewis, S. J. (2010). The specific contributions of set-shifting to freezing of gait in Parkinson's disease. *Movement Disorders, 25*(8), 1000–1004. https://doi.org/10.1002/mds.23005.

Nitschke, K., Kostering, L., Finkel, L., Weiller, C., & Kaller, C. P. (2017). A meta-analysis on the neural basis of planning: Activation likelihood estimation of functional brain imaging results in the tower of London task. *Human Brain Mapping, 38*(1), 396–413. https://doi.org/10.1002/hbm.23368.

Nonnekes, J., Snijders, A. H., Nutt, J. G., Deuschl, G., Giladi, N., & Bloem, B. R. (2015). Freezing of gait: A practical approach to management. *Lancet Neurology, 14*(7), 768–778. https://doi.org/10.1016/S1474-4422(15)00041-1.

Nutt, J. G., Bloem, B. R., Giladi, N., Hallett, M., Horak, F. B., & Nieuwboer, A. (2011). Freezing of gait: Moving forward on a mysterious clinical phenomenon. *Lancet Neurology, 10*(8), 734–744. https://doi.org/10.1016/s1474-4422(11)70143-0.

Ogawa, S., & Lee, T. M. (1990). Magnetic resonance imaging of blood vessels at high fields: In vivo and in vitro measurements and image simulation. *Magnetic Resonance in Medicine, 16*(1), 9–18. https://doi.org/10.1002/mrm.1910160103.

Pan, P., Zhang, Y., Liu, Y., Zhang, H., Guan, D., & Xu, Y. (2017). Abnormalities of regional brain function in Parkinson's disease: A meta-analysis of resting state functional magnetic resonance imaging studies. *Scientific Reports, 7*, 40469. https://doi.org/10.1038/srep40469.

Pereira, F., Mitchell, T., & Botvinick, M. (2009). Machine learning classifiers and fMRI: A tutorial overview. *Neuroimage, 45*(1), S199–S209. https://doi.org/10.1016/j.neuroimage.2008.11.007.

Prodoehl, J., Spraker, M., Corcos, D., Comella, C., & Vaillancourt, D. (2010). Blood oxygenation level dependent activation in basal ganglia nuclei relates to specific symptoms in De novo Parkinson's disease. *Movement Disorders, 25*(13), 2035–2043. https://doi.org/10.1002/mds.23360.

Ricciardi, L., Bloem, B. R., Snijders, A. H., Daniele, A., Quaranta, D., Bentivoglio, A. R., & Fasano, A. (2014). Freezing of gait in Parkinson's disease: The paradoxical interplay between gait and cognition. *Parkinsonism & Related Disorders, 20*(8), 824–829. https://doi.org/10.1016/j.parkreldis.2014.04.009.

Rodriguez-Oroz, M. C., Jahanshahi, M., Krack, P., Litvan, I., Macias, R., Bezard, E., & Obeso, J. A. (2009). Initial clinical manifestations of Parkinson's disease: Features and pathophysiological mechanisms. *Lancet Neurology, 8*(12), 1128–1139. https://doi.org/10.1016/s1474-4422(09)70293-5.

Salvador, R., Martinez, A., Pomarol-Clotet, E., Gomar, J., Vila, F., Sarro, S., Capdevila, A., & Bullmore, E. (2008). A simple view of the brain through a frequency-specific functional connectivity measure. *Neuroimage, 39*(1), 279–289. https://doi.org/10.1016/j.neuroimage.2007.08.018.

Shine, J. M., Matar, E., Ward, P. B., Frank, M. J., Moustafa, A. A., Pearson, M., Naismith, S. L., & Lewis, S. J. (2013). Freezing of gait in Parkinson's disease is associated with functional decoupling between the cognitive control network and the basal ganglia. *Brain, 136*(Pt 12), 3671–3681. https://doi.org/10.1093/brain/awt272.

Skidmore, F. M., Yang, M., Baxter, L., von Deneen, K. M., Collingwood, J., He, G., White, K., Korenkevych, D., Savenkov, A., Heilman, K. M., Gold, M., & Liu, Y. (2013). Reliability analysis of the resting state can sensitively and specifically identify the presence of Parkinson disease. *Neuroimage, 75*, 249–261. https://doi.org/10.1016/j.neuroimage.2011.06.056.

Snijders, A. H., Takakusaki, K., Debu, B., Lozano, A. M., Krishna, V., Fasano, A., Aziz, T. Z., Papa, S. M., Factor, S. A., & Hallett, M.

(2016). Physiology of freezing of gait. *Annals of Neurology, 80*(5), 644–659. https://doi.org/10.1002/ana.24778.

Tahmasian, M., Eickhoff, S.B., Giehl, K., Schwartz, F., Herz, D.M., Drzezga, A., van Eimeren, T., Laird, A.R., Fox, P.T., Khazaie, H., Zarei, M., Eggers, C., Eickhoff, C.R. Resting-state functional reorganization in Parkinson's disease: An activation likelihood estimation meta-analysis. Cortex 2017; 92: 119–138. https://doi.org/10.1016/j.cortex.2017.03.016.

Tessitore, A., Amboni, M., Esposito, F., Russo, A., Picillo, M., Marcuccio, L., Pellecchia, M. T., Vitale, C., Cirillo, M., Tedeschi, G., & Barone, P. (2012). Resting-state brain connectivity in patients with Parkinson's disease and freezing of gait. *Parkinsonism & Related Disorders, 18*(6), 781–787. https://doi.org/10.1016/j.parkreldis.2012.03.018.

van Buuren, M., Gladwin, T. E., Zandbelt, B. B., van den Heuvel, M., Ramsey, N. F., Kahn, R. S., & Vink, M. (2009). Cardiorespiratory effects on default-mode network activity as measured with fMRI. *Human Brain Mapping, 30*(9), 3031–3042. https://doi.org/10.1002/hbm.20729.

Vandenbossche, J., Deroost, N., Soetens, E., Spildooren, J., Vercruysse, S., Nieuwboer, A., & Kerckhofs, E. (2011). Freezing of gait in Parkinson disease is associated with impaired conflict resolution. *Neurorehabilitation and Neural Repair, 25*(8), 765–773. https://doi.org/10.1177/1545968311403493.

Vercruysse, S., Spildooren, J., Heremans, E., Wenderoth, N., Swinnen, S. P., Vandenberghe, W., & Nieuwboer, A. (2014). The neural correlates of upper limb motor blocks in Parkinson's disease and their relation to freezing of gait. *Cerebral Cortex, 24*(12), 3154–3166. https://doi.org/10.1093/cercor/bht170.

Vervoort, G., Heremans, E., Bengevoord, A., Strouwen, C., Nackaerts, E., Vandenberghe, W., & Nieuwboer, A. (2016). Dual-task-related neural connectivity changes in patients with Parkinson' disease. *Neuroscience, 317*, 36–46. https://doi.org/10.1016/j.neuroscience.2015.12.056.

Visser, M., Jefferies, E., Embleton, K. V., & Lambon Ralph, M. A. (2012). Both the middle temporal gyrus and the ventral anterior temporal area are crucial for multimodal semantic processing: Distortion-corrected fMRI evidence for a double gradient of information convergence in the temporal lobes. *Journal of Cognitive Neuroscience, 24*(8), 1766–1778. https://doi.org/10.1162/jocn_a_00244.

Wu, T., & Hallett, M. (2013). The cerebellum in Parkinson's disease. *Brain, 136*(Pt 3), 696–709. https://doi.org/10.1093/brain/aws360.

Xue, S., Wang, X., Wang, W., Liu, J., & Qiu, J. (2016). Frequency-dependent alterations in regional homogeneity in major depression. *Behavioural Brain Research, 306*, 13–19. https://doi.org/10.1016/j.bbr.2016.03.012.

Yang, H., Long, X. Y., Yang, Y., Yan, H., Zhu, C. Z., Zhou, X. P., Zang, Y. F., & Gong, Q. Y. (2007). Amplitude of low frequency fluctuation within visual areas revealed by resting-state functional MRI. *Neuroimage, 36*(1), 144–152. https://doi.org/10.1016/j.neuroimage.2007.01.054.

Zach, H., Janssen, A. M., Snijders, A. H., Delval, A., Ferraye, M. U., Auff, E., Weerdesteyn, V., Bloem, B. R., & Nonnekes, J. (2015). Identifying freezing of gait in Parkinson's disease during freezing provoking tasks using waist-mounted accelerometry. *Parkinsonism & Related Disorders, 21*(11), 1362–1366. https://doi.org/10.1016/j.parkreldis.2015.09.051.

Zang, Y. F., He, Y., Zhu, C. Z., Cao, Q. J., Sui, M. Q., Liang, M., Tian, L. X., Jiang, T. Z., & Wang, Y. F. (2007). Altered baseline brain activity in children with ADHD revealed by resting-state functional MRI. *Brain & Development, 29*(2), 83–91. https://doi.org/10.1016/j.braindev.2006.07.002.

Zhong, M., Yang, W., Huang, B., Jiang, W., Zhang, X., Liu, X., Wang, L., Wang, J., Zhao, L., Zhang, Y., Liu, Y., Lin, J., & Huang, R. (2018). Effects of levodopa therapy on voxel-based degree centrality in Parkinson's disease. *Brain Imaging and Behavior*. https://doi.org/10.1007/s11682-018-9936-7.

Zhu, W., Fu, X., Cui, F., Yang, F., Ren, Y., Zhang, X., Zhang, X., Chen, Z., Ling, L., & Huang, X. (2015). ALFF value in right Parahippocampal gyrus acts as a potential marker monitoring amyotrophic lateral sclerosis progression: A neuropsychological, voxel-based morphometry, and resting-state functional MRI study. *Journal of Molecular Neuroscience, 57*(1), 106–113. https://doi.org/10.1007/s12031-015-0583-9.

Zuo, X. N., Di Martino, A., Kelly, C., Shehzad, Z. E., Gee, D. G., Klein, D. F., Castellanos, F. X., Biswal, B. B., & Milham, M. P. (2010). The oscillating brain: Complex and reliable. *Neuroimage, 49*(2), 1432–1445. https://doi.org/10.1016/j.neuroimage.2009.09.037.